TO BE SUBMITTED
TO NUOVO CIMENTO

CERN/TC/PHYSICS 66-22
23.8.1966.

EXPERIMENTAL RESULTS ON $\bar{p}p$ ANNIHILATIONS AT 1.2 GeV/c WITH PRODUCTION OF AT LEAST ONE K_1^o MESON

J. Barlow, E. Lillestøl, L. Montanet, L. Tallone-Lombardi,
CERN, Genève

C. d'Andlau, A. Astier, L. Dobrzynski, S. Wojcicki,
Laboratoire de Physique Nucléaire, Collège de France, Paris

A.M. Adamson, J. Duboc, F. James, M. Goldberg,
Institut du Radium, Paris

R.A. Donald, R. James, J.E.A. Lys, T. Nisar,
Nuclear Physics Research Laboratories, Liverpool

PS/5600/rmn

ABSTRACT

We present results on annihilations of antiprotons at 1.2 GeV/c into two, three and four body final states including at least one visible K_1^o.

The three and four body channels are dominated by $K^*(891)$.

Resonances in the $K\bar{K}$ and $K\bar{K}\pi$ systems are discussed and cross-sections are given.

It is found that at 1.2 GeV/c it is no longer true that annihilation occurs predominantly from S-states.

1. Introduction

In this paper, we present the results of an analysis of the following 1.2 GeV/c $\bar{p}p$ annihilation channels :

2-body channels: $\bar{p}p \rightarrow K_1^0 K_1^0$

$\bar{p}p \rightarrow K_1^0 K_2^0$

3-body channels: $\bar{p}p \rightarrow K_1^0 K_1^0 \pi^0$

$\bar{p}p \rightarrow K_1^0 K^{\pm} \pi^{\mp}$

4-body channels: $\bar{p}p \rightarrow K_1^0 K_1^0 \pi^+ \pi^-$

$\bar{p}p \rightarrow K_1^0 K_2^0 \pi^+ \pi^-$

$\bar{p}p \rightarrow K_1^0 K^{\pm} \pi^{\mp} \pi^0$

For the 5 and 6-body channels, we refer to the publication by C. d'Andlau et al.[1] where the evidence for the existence of the $D^0(1290)$ meson was proposed.

The analysis of the 2-body channels shows that 1.2 GeV/c $\bar{p}p$ annihilations occur not only in S-states, which are known to be predominant in annihilations at rest, but also in higher angular momentum states, the contribution of these higher angular momentum states being at least as large as those of the S-states.

For each channel, we give the total cross-section. We also give the production cross-sections for $K^{*}(891)$, $\rho(765)$, and $\varphi(1020)$ resonances, as well as evidence for possible resonances decaying into $K\bar{K}$ and $K\bar{K}\pi$ at :

$M\ (K_1^0 K_1^0) = 1045$ MeV, 1255 MeV

$M\ (K_1^0 K^{\pm}) = 1325$ MeV

$M\ (K_1^0 K^{\pm} \pi^{\mp}) = 1290$ MeV

None of these four possible resonances has to be considered as an evidence for a new resonance, since each of them may be compared with already

known effects: $K_1^oK_1^o(1068)$, $f^o(1250)$, $A_2(1310)$, and $D^o(1290)$.

We also show that we need to introduce an S-wave scattering length of 2.5 ± 0.5 Fermi (zero effective range approximation) to interpret the $K_1^oK^\pm$ mass spectrum near $K_1^oK^\pm$ threshold in the 4-body annihilations.

On the other hand, we do not find any ($K\pi\pi$) enhancements: in particular, the $C^o(1230)$ enhancement which was observed in 4-body annihilations at rest[2] do not appear to be produced at 1.2 GeV/c.

The results were obtained from an analysis of $\bar{p}p$ annihilations involving at least one visible K_1^o decay. The film under study was taken in the Saclay 81 cm HBC exposed to a beam of $1.18 \pm .01$ GeV/c $\bar{p}$ from the Cern PS. The results presented correspond to the complete film sample of 3.4×10^6 $\bar{p}$.

Each event was weighted in order to correct for the finite probability of the K_1^o to decay outside the visible region of the chamber and for the probability that the K_1^o decays within 0.2 cm from the production apex. These weights were used when necessary in the following analysis, in particular for the calculation of the cross-sections, for which we have also taken into account the neutral decay mode of the K_1^o and the scanning efficiency.

2. Two body annihilations

The analysis of 797 zero-prong annihilations associated with one or two observed K_1^o provides the following results :

(1) $\bar{p}p \rightarrow K_1^oK_1^o$ 8 ev^{ts} $\sigma = (5.9 \pm 2.3)$ μb

(2) $\bar{p}p \rightarrow K_1^o(K^o)$ 67 ev^{ts}

Fig. 1 shows the missing mass squared spectrum for all 0 prong 1 V^o events. The contamination from other channels is estimated to be less than 10 o/o for these reactions.

Reaction (2) is composed of two different types of annihilations:

$\bar{p}p \to K_1^oK_2^o$ and $\bar{p}p \to K_1^oK_1^o$ in which one K_1^o is not observed. The comparison of reaction (1) and (2) leads to the following results for $\bar{p}p \to K_1^oK_2^o$:

(3) $\bar{p}p \to K_1^oK_2^o$ $\sigma = (17 \pm 5)$ μb

These results are significantly different from those obtained at rest[3] for which the ratio:

$$(\bar{p}p \to K_1^oK_1^o) / (\bar{p}p \to K_1^oK_2^o)$$

was found to be less than 1/333. It was concluded from this result that annihilations at rest occur mainly in S-states, the upper limit for the ratio P-wave / S-wave being 10 o/o at 90 o/o confidence level[4]. This conclusion is no valid for $\bar{p}p$ annihilations at 1.2 GeV/c; the results for reaction (1) show that angular momentum states other than S-states are present in the annihilation. The comparison of the cross-sections for reaction (1) and (3) indicates that the contribution of higher angular momentum states is important.

The angular distribution of the K^o has been folded about 90^o in the centre of mass system and fitted to a $\cos^{2n}\theta$ series. The third and higher terms are not required to get a good fit: therefore we cannot obtain any further information about the initial angular momentum states.

3. Three body annihilations

The following reactions have been studied :

(4) $\bar{p}p \to K^+K_1^o\pi^-$ 375 ev^{ts} $\sigma = (128 \pm 10)$ μb

(5) $\bar{p}p \to K^-K_1^o\pi^+$ 365 ev^{ts} $\sigma = (124 \pm 10)$ μb

(6) $\bar{p}p \to K_1^oK_1^o\pi^o$ 92 ev^{ts} $\sigma = (59 \pm 7)$ μb

The contamination from other channels is less than 1 o/o for reactions (4) and (5) and less than 5 o/o for reaction (6).

Consider first reactions (4) and (5): Fig. 2 shows the Dalitz plot of the effective mass squared for the 740 events. There are well defined

bands corresponding to the $K^{*}(891)$ resonances, and also possible bands corresponding to a $K\bar{K}$ resonance around 1320 MeV and/or a $K\pi$ resonance at 1400 MeV.

The distribution of points on the Dalitz plot is fitted using the method of maximum likelihood. Since annihilations from higher angular momentum states than S-states are important, a correct matrix element to describe the interaction is not easily constructed. The fits presented here have been carried out using a simple matrix element assuming no interference effects.

The function used for the fits is of the form:

$$D = \left\{ \sum_i f_i F_i A_i + 1 - \sum_i f_i \right\}$$

where the f_i are the fractions of the appropriate resonances, the A_i are normalization factors of the form:

$$A_i = \frac{\int dM^2 (K^{\pm}\pi^{\mp})\, dM^2 (K^{o}\pi^{\pm})}{\int F_i\, dM^2 (K^{\pm}\pi^{\mp})\, dM^2 (K^{o}\pi^{\pm})}$$

and

$$F_i = \frac{\Gamma_i}{(m_i^2 - m_{io}^2)^2 + m_{io}^2 \Gamma_i^2}$$

where m_i^2 is the effective mass squared of the appropriate two particle combination, m_{io}^2 is the effective mass squared and Γ_i the width of the resonance.

Using this density function, four possibilities were tested:

A) that only the $K^{*}(891)$ resonances are produced,

B) that only the $K^{*}(891)$ and the $K\bar{K}(1320)$ resonances are produced,

C) that only the $K^{*}(891)$ and the $K\pi(1400)$ resonances are produced,

D) that $K^{*}(891)$, $K\bar{K}(1320)$ and $K\pi(1400)$ are produced.

Preliminary fits using these density functions were not sensitive to the masses and widths of the $K\bar{K}(1320)$ and the $K\pi(1400)$ enhancements. We therefore tested the hypothesis that these enhancements could be compatible

with the A_2 and $K^*(1400)$ by fixing the mass and width at 1310 MeV and 80 MeV for the $K\bar{K}$ enhancement and at 1410 MeV and 100 MeV for the $K\pi$ enhancement. The results of these fits are tabulated below.

TABLE I

		$K^{*o}(891)$	$K^{*\pm}(891)$	$K\bar{K}(1320)$	$K^{*o}(1400)$	$K^{*\pm}(1400)$	
	M	899 ± 4	890 ± 3				MeV
A	Γ	33 ± 8	42 ± 7				MeV
	f	13.5 ± 2.2	27 ± 3.0				o/o
	M	898 ± 4	890 ± 3	1310			MeV
B	Γ	34 ± 8	45 ± 7	80			MeV
	f	14 ± 2.3	28.2 ± 2.8	7.8 ± 2.4			o/o
	M	900 ± 4	890 ± 3		1410	1410	MeV
C	Γ	37 ± 9	45 ± 7		100	100	MeV
	f	15.0 ± 2.4	28.3 ± 2.9		6.0 ± 2.6	5.3 ± 2.5	o/o
	M	899 ± 4	890 ± 3	1310	1410	1410	MeV
D	Γ	37 ± 9	47 ± 7	80	100	100	MeV
	f	15.1 ± 2.4	29.1 ± 2.9	6.5 ± 2.5	4.3 ± 2.3	4.0 ± 2.5	o/o

The probabilities of these four fits are acceptable but not significantly different. However, the solution corresponding to hypothesis (B) is preferred because of the comparison with the three mass spectra $M^2(K^{\pm}\pi^{\mp})$, $M^2(K^o_1,\pi^{\pm})$, $M^2(K^{\pm}K^o_1)$, (Fig. 3).

Moreover, the angular distribution of the K^o_1 in the rest frame of the $K\bar{K}$ system with respect to the normal to the production plane shows a striking anisotropy for the events inside the $K\bar{K}(1320)$ enhancement, when the same angular distribution is flat for events outside of $K\bar{K}(1320)$ enhancement (Fig. 4).

To obtain a cleaner distribution, events for which the ($K\pi$) effective mass falls in the $K^{*}(891)$ band: $0.74\ GeV^2 < M^2(K\pi) < 0.84\ GeV^2$ have been removed.

A similar study of the decay angular distribution of the $K\pi$ system around 1400 MeV shows no deviation from isotropy.

We then conclude that our data for reactions (4) and (5) indicate a large production of $K^{*}(891)$ and a small but significant production of $K\bar{K}(1320)$ resonance.

In view of these results, we have tried again solution (B), with the mass, width and percentage of all three resonances $K^{*\pm}(891)$, $K^{*o}(891)$, $K\bar{K}(1320)$ as free parameters: Table II gives the results of the fit:

TABLE II

	$K^{*o}(891)$	$K^{*\pm}(891)$	$K\bar{K}(1320)$
Mass(MeV)	899 ± 4	890 ± 3	1333 ± 13
Width(MeV)	34 ± 8	44 ± 7	56 ± 28
f (o/o)	14 ± 3	28 ± 3	7.5 ± 3

The corresponding cross-sections for the two body processes: $\bar{p}p \to K^{*o}K_1^o$, $\bar{p}p \to K^{*\pm}K^{\mp}$ and $\bar{p}p \to K\bar{K}(1320)\,\pi^{\pm}$ when K^{*o} decay into $K^{\pm}\pi^{\mp}$ and $K^{*\pm}$ into $K_1^o\pi^{\pm}$ are then:

$\bar{p}p \to K^{*o}K_1^o$ $\qquad \sigma = (35 \pm 6)\ \mu b$

$\bar{p}p \to K^{*\pm}K^{\mp}$ $\qquad \sigma = (70 \pm 7)\ \mu b$

$\bar{p}p \to K\bar{K}(1320)\,\pi^{\mp}$ $\qquad \sigma = (19 \pm 7)\ \mu b$

We next consider the production properties of the $K^{*}(891)$. For this purpose events were selected by demanding: $0.74\ GeV^2 < M^2(K\pi) < 0.84\ GeV^2$.

Fig. (5) shows the $\cos\theta$ distribution of the $K^{*}(891)$ in the production centre of mass system. Defining forward for the $\bar{K}^{*}$ to be the direction

of the $\bar{p}$ and for the K^{*} the direction of the p we tabulate the forward/total ratio of the K^{*} charged and K^{*} neutral :

$$K^{*\pm} \quad : \quad 0.61 \pm 0.04$$

$$K^{*o} \quad : \quad 0.56 \pm 0.05 \quad .$$

This is a ~ 3 standarddeviations evidence that the final state $K^{*}K$ is asymmetric in the production center of mass system, the $\bar{K}^{*}$ prefering the direction of the $\bar{p}$ and K^{*} the direction of the p. The asymmetry disappears outside the K^{*} band.

This asymmetry is again evidence for initial states other than S-states being important in the annihilation process at 1.2 GeV/c.

An attempt was made to obtain information on the production process by examining the spin density matrix elements of the $K^{*}(890)$. No deviations from pure phase space productions were found.

We now consider the reaction : $\bar{p}p \rightarrow K_1^o K_1^o \pi^o$

The folded Dalitz plot for the $K\pi$ combinations is shown in Fig. (6).

The non uniformity of the points together with the relatively small number of events make the fitting of this Dalitz plot difficult. However, we have verified that taking into account a reasonable $C = +1/C = -1$ ratio for the $\bar{K}^{*}K$ production in the $K_1^o K^{\pm} \pi^{\mp}$ channel, the number of events found in the K^{*} bands for $K_1^o K_1^o \pi^o$ final state is in agreement with the number of K^{*}'s fitted in the charged channel.

4. Four body annihilations

The following reactions have been studied:

(7) $\bar{p}p \rightarrow K_1^o K_1^o \pi^+ \pi^-$ 397 ev^{ts} $\sigma = (208 \pm 20)$ μb

(8) $\bar{p}p \rightarrow K_1^o (K^o) \pi^+ \pi^-$ 864 ev^{ts}

(9) $\bar{p}p \rightarrow K_1^o K^\pm \pi^\mp \pi^o$ 1621 ev^{ts} $\sigma = (590 \pm 25)$ μb

In reaction (7), both K_1^o give a visible $\pi^+\pi^-$ decay. The contamination from other channels is less than 1 o/o.

Figure 7 shows the effective mass squared distributions for the combinations Kπ, ππ, $K\bar{K}$. The Kπ distribution shown is the sum of the four possible combinations. The solid curves are obtained from a maximum likelihood fit to the channel as a whole, using matrix elements yielding the density :

$$\alpha \ |T_1|^2 + \beta \ |T_2|^2 + \text{const.} \ (1-\alpha-\beta)$$

where α is the percentage of $K^*(891)$ production, β is the percentage of ρ(765) production and the terms T represent amplitudes for $K^*(891)$ and ρ(765).[5]

This simple matrix element is sufficient to give good fits of the Kπ and ππ distributions, but not of the $K_1^o K_1^o$ distribution in which can be seen two possible enhancements at $M^2(K_1^o K_1^o) \sim 1.02$ GeV^2 and 1.60 GeV^2. (On the Kπ spectrum, one may notice an enhancement at $M^2(K\pi) \sim .56$ GeV^2, i.e. in the vicinity of the K(725) meson, but this effect does not show up in the other (Kπ) spectra we present below, so that we interpret it as a statistical fluctuation of the data).

Since reaction (7) is dominated by $K^*(891)$ production, an attempt was made to remove some of the background in the $K_1^o K_1^o$ distribution due to $K^*(891)$ production by removing those events for which at least one Kπ effective mass falls within the range defined by:

$$0.74 \text{ GeV}^2 < M^2(K\pi) < 0.84 \text{ GeV}^2 \ .$$

The result is illustrated in Fig. (7d). An attempt was made to fit this selected $K_1^oK_1^o$ distribution using Monte-Carlo techniques to determine the background. The solid curve α is the result of a fit with two Breit-Wigner amplitudes centred around the two enhancements. Clearly, this fit, although acceptable (probability = 34 o/o), does not reproduce completely the absence of events in the gap between the two enhancements: this may be due to some interference effects not considered in the present analysis, or due to an excess of events in the mass region around 1430 MeV. Our statistically limited data does not allow us to clarify this point, but the two enhancements at 1.02 and 1.60 GeV^2 may be more significant than it appears from the results of the fit given in Table III.(6)

An attempt was made to interpret the lower $K_1^oK_1^o(1040)$ enhancement with a zero effective range approximation for a $K_1^oK_1^o$ S-wave scattering effect(7). A poor fit (curve β) was obtained with an indeterminate value for the $K_1^oK_1^o$ S-wave scattering length ($a = 9 \,^{+\,62}_{-\,\,9}$ fermi).

The results from the fits performed are summarized in Table III. The percentages given for the $K_1^oK_1^o$ enhancements have been corrected for the cuts made on the $K\pi$ distributions.

TABLE III

$\bar{p}p \to K_1^oK_1^o\pi^+\pi^-$	o/o	Mass (MeV)	Width (MeV)	Production cross-section (μb)
$K^*(891)$	57 ± 7	890 ± 3	43 ± 9	118 ± 18
$\rho(765)$	25 ± 8	745 ± 9	92 ± 42	52 ± 15
$K_1^oK_1^o(1045)$	12 ± 4	1045 ± 9	50 ± 24	25 ± 10
$K_1^oK_1^o(1260)$	20 ± 7	1255 ± 13	82 ± 34	41 ± 15

In reaction (8), one K^o is not observed. The contamination from other channels is less than 3 o/o.

This channel is composed of approximately equal amounts of $K_1^oK_1^o$ and $K_1^oK_2^o$ events. A similar analysis to the one described above was carried out.

The two body effective mass squared distributions are shown in Fig. 8: once more, $K^*(891)$ production is seen to dominate the channel with a relatively small but significant $\rho(765)$ production. These results are compatible with 100 o/o of $K^*(891)$ production and no production of $\rho(765)$ for the reaction $\bar{p}p \rightarrow K_1^oK_2^o\pi^+\pi^-$.

A cut was made on the $K\pi$ effective mass in order to provide a "cleaner" $K\bar{K}$ distribution: the resulting $K\bar{K}$ spectrum is shown in Fig. 8d. In addition to effects coming from the $K_1^oK_2^o$ component, this channel should contain the same resonances as were found for reaction(7). The amounts found for these resonances are compatible with the results for reaction (7). An effect of the $K_1^oK_2^o$ component is readily seen near threshold where the $\varphi(1020)$ is clearly produced. A maximum likelihood analysis gives for the production of the φ meson:

$$M(\varphi) = 1019 \pm 3 \text{ MeV} \qquad \Gamma(\varphi) = 10 \pm 3 \text{ MeV}$$

$$\sigma(\bar{p}p \rightarrow \varphi\pi^+\pi^- \text{ with } \varphi \rightarrow K_1^oK_2^o) = (12 \pm 3)\ \mu b\ .$$

In view of obvious statistical limitations, we do not attempt to give a more detailed analysis of this channel.

In reaction (9), the contamination from other channels is less than 3 o/o.

As in reaction (7), a likelihood analysis of the channel as a whole was made with a matrix-element taking into account $K^*(891)$ and $\rho(765)$ production.

The two body effective mass squared distributions are shown in Fig. 9 together with the fitted curves. While a good fit was obtained for the $K\pi$ distributions, poor fits were obtained for $(\pi\pi)$ and $(K\bar{K})$ distributions.

In the latter, two possible enhancements at $M^2(K^{\pm}K^0_1) \sim 1.2$ GeV^2 and 1.75 GeV^2 can be seen.

Using the same technique as described above, K^* events were preferentially removed, leaving a cleaner $K\bar{K}$ spectrum (Fig. 9e).

Two fits were performed to this spectrum:

a) introduction of a zero effective range approximation S-wave scattering amplitude[6] and a Breit-Wigner amplitude at a mass value $\sim$ 1320 MeV.

b) Two Breit-Wigner amplitudes at mass values $\sim$ 1000 MeV and 1320 MeV.

The fit (b) is not significantly better than fit (a); it thus seems that the enhancement at threshold can be very well explained with an S-wave scattering length of

$$a = (2.5 \pm 0.5) \text{ Fermi} .$$

The inclusion of the reflexion of this effect improves the fit of the $(\pi\pi)$ spectrum. The results from the fits performed on reaction (8) are summarized in Table IV:

TABLE IV

$\bar{p}p \rightarrow K^0_1 K^{\pm}\pi^{\mp}\pi^0$	o/o	Mass (MeV)	Width (MeV)	Production cross-section (μb)
$K^{*\pm}(891)$	37 ± 3	889 ± 3	53 ± 7	220 ± 22
$K^{*0}(891)$	19 ± 3	897 ± 4	53 ± 13	113 ± 18
$\rho(765)$	20 ± 4	730 ± 11	130 ± 25	119 ± 22
$(K\bar{K})^{\pm}$ (Threshold)	2.4 ± 0.5 Fermi			95 ± 20
$(K\bar{K})^{\pm}$ (1320)	5 ± 2	1317 ± 3	56 ± 15	30 ± 12

5. $(K\bar{K}\pi)$ and $(K\pi\pi)$ systems in $\bar{p}p \rightarrow K\bar{K}\pi\pi$

No three body $(K\pi\pi)$ enhancements have been observed in the 4-body annihilations (7), (8), (9), neither on the overall $(K\pi\pi)$ spectra, nor on the selected events when $K^{*}(891)$ or $\rho(765)$ were produced. In particular, the C(1230) enhancement which was observed in four body annihilations at rest[2] do not appear to be produced at 1.2 GeV/c.

No three body $(K\bar{K}\pi)$ enhancements were observed in the reactions (7) and (8), where only charged $(K\bar{K}\pi)$ combinations exist. On the other hand, for reaction (9), the neutral $(K\bar{K}\pi)$ spectrum is different from the charged $(K\bar{K}\pi)$ one, in particular when one selects events with $M^2(K\bar{K}) < 1.05$ GeV^2 (Fig. 10).

The main difference comes from an excess of events in the neutral $(K\bar{K}\pi)$ combinations, around $M^2(K\bar{K}\pi) \sim 1.65$ GeV.

This enhancement may be interpreted as evidence for the production of the $D^0(1290)$ meson, which has been shown to be produced in the 5 and 6-body annihilations at 1.2 GeV/c. A fit to the experimental distribution, using Monte-Carlo techniques to determine the background and assuming for the D^0 meson a mass of 1290 MeV and a width of 25 MeV gives:

$$\bar{p}p \rightarrow D^0\pi^0 \text{ with } D^0 \rightarrow K^0_1 K^{\pm}\pi^{\mp} = 19 \pm 5 \text{ events}$$

(cross-section $\sigma = 7 \pm 2$ μb)

6. Conclusions

There is evidence for resonances in the $K\bar{K}$ system at $M(K\bar{K})$=1045 MeV, 1250 MeV and 1320 MeV. The fact that the resonances at 1045 and 1250 MeV are not observed in the charged $(K\bar{K})$ system indicates that there are isoscalars. The $K\bar{K}(1320)$ resonances observed in the three and four body reactions are probably a single resonance with T = 1; with the statistics of our experiment, we do not expect to observe the neutral member of the triplet.

In Table V, we assemble for convenience the cross-sections for the reactions studied.

TABLE V

Reaction:	Cross-section (μb):
$\bar{p}p \rightarrow K_1^0 K_1^0$	5.9 ± 2.3
$\bar{p}p \rightarrow K_1^0 K_2^0$	17 ± 5
$\bar{p}p \rightarrow K^{*0} K^0$	105 ± 18
$\bar{p}p \rightarrow K^{*\pm} K^{\mp}$	210 ± 20
$\bar{p}p \rightarrow K\bar{K}(1320)\pi^{\pm}$	38 ± 14
$\bar{p}p \rightarrow D^0 \pi^0$	14 ± 4
$\bar{p}p \rightarrow K_1^0 K_1^0 \pi^0$	50 ± 7
$\bar{p}p \rightarrow K^0 K^{\mp} \pi^{\pm}$	252 ± 20
$\bar{p}p \rightarrow K^{*0} K^{\mp} \pi^{\pm}$	226 ± 36
$\bar{p}p \rightarrow K^{*\pm} K^{\mp} \pi^0$	247 ± 40
$\bar{p}p \rightarrow K^{*\pm} K^0 \pi^{\mp}$	579 ± 80
$\bar{p}p \rightarrow K^0 K^0 \rho^0$	104 ± 30
$\bar{p}p \rightarrow K\bar{K}(1045)\pi^+\pi^-$	50 ± 20
$\bar{p}p \rightarrow K\bar{K}(1250)\pi^+\pi^-$	82 ± 30
$\bar{p}p \rightarrow K\bar{K}(1320)\pi^{\pm}\pi^0$	60 ± 24
$\bar{p}p \rightarrow K_1^0 K_1^0 \pi^+\pi^-$	~ 0
$\bar{p}p \rightarrow K_1^0 K_2^0 \pi^+\pi^-$	~ 0
$\bar{p}p \rightarrow K^0 K^{\mp} \pi^{\pm} \pi^0$	~ 0

In the table, the symbol K^0 assumes an equal number of K_1^0 and K_2^0, the symbols K^{*0} and $K^{*\pm}$ include all decay-modes.

FIGURE CAPTIONS

Fig. 1 Missing mass squared spectrum for 0 prong 1 V^0 events. The peak at the low mass squared is centred at the value corresponding to the K^0.

Fig. 2 Dalitz plot in effective mass squared for the reaction: $\bar{p}p \to K_1^0 K^{\pm} \pi^{\mp}$.

Fig. 3 Projections of Fig. 2 on the $M^2(K^{\pm}\pi^{\mp})$, $M^2(K_1^0\pi^{\pm})$ and $M^2(K_1^0 K^{\pm})$ axes.

In Fig. 3a and b, the curve represents the best prediction.

In Fig. 3c, curves α and β correspond respectively to the solutions (a) and (b). (see text).

Fig. 4 Angular distribution of the K_1^0 in the rest frame of the $K\bar{K}$ system with respect to the normal to the production plane for the reaction $\bar{p}p \to K_1^0 K^{\pm} \pi^{\mp}$.

The distributions have been folded about 90^0.

Histograms (a), (b) and (c) correspond respectively to the following mass squared regions:

(a): $1.2\ \text{GeV}^2 < M^2(K\bar{K}) < 1.6\ \text{GeV}^2$

(b): $1.6\ \text{GeV}^2 < M^2(K\bar{K}) < 2.0\ \text{GeV}^2$

(c): $2.0\ \text{GeV}^2 < M^2(K\bar{K}) < 2.4\ \text{GeV}^2$

Fig. 5 Angular distribution of the K^* in the production centre of mass system for reaction $\bar{p}p \to K_1^0 K^{\pm} \pi^{\mp}$.

Fig. 5a refers to K^{*0}; Fig. 5b refers to $K^{*\pm}$.

Fig. 6 Dalitz plot in effective mass squared for the reaction: $\bar{p}p \to K_1^0 K_1^0 \pi^0$.

Fig. 7 $\bar{p}p \to K_1^0 K_1^0 \pi^+ \pi^-$ (397 events).

Fig. 7a: effective mass squared spectrum of the two body ($K\pi$) system (4 combinations per event).

Fig. 7b: effective mass squared spectrum of the two body ($\pi\pi$) system.

Fig. 7c: effective mass squared spectrum of the two body ($K_1^0 K_1^0$) system.

The curves on Fig. 1a, b and c correspond to the fit obtained when assuming $K^{*}(891)$, $\rho(765)$ and phase space contributions.

Fig. 7d: effective mass squared spectrum of the two body $(K_1^oK_1^o)$ system when $M^2(K\pi) > 0.837$ GeV^2 or $M^2(K\pi) < 0.748$ GeV^2.

Curve α corresponds to the fit of two Breit-Wigner amplitudes at $M^2(K_1^oK_1^o) = 1.02$ GeV^2 and $M^2(K_1^oK_1^o) = 1.60$ GeV^2 plus phase-space.

Curve β corresponds to the fit of an S-wave scattering length at threshold and a Breit-Wigner amplitude at $M^2(K_1^oK_1^o) = 1.60$ GeV^2.

Fig. 8 $\bar{p}p \rightarrow K_1^o(K^{\bullet})\pi^+\pi^-$ (864 events).

Fig. 8a: effective mass squared spectrum of the two body $(K\pi)$ system (4 combinations per event).

Fig. 8b: effective mass squared spectrum of the two body $(\pi\pi)$ system.

Fig. 8c: effective mass squared spectrum of the two body $(K_1^oK_1^o)$ system.

Fig. 8d: effective mass squared spectrum of the two body $(K_1^oK_1^o)$ system when $M^2(K\pi) > 0.837$ GeV^2 or $M^2(K\pi) < 0.748$ GeV^2.

The curves correspond to the fit obtained when assuming $K^{*}(891)$, $\rho(765)$ and phase-space contributions.

Fig. 9 $\bar{p}p \rightarrow K_1^oK^{\pm}\pi^{\mp}\pi^o$ (1621 events).

Fig. 9a: effective mass squared spectrum of the two body $(K\pi)^{\pm}$ system (2 combinations per event).

Fig. 9b: effective mass squared spectrum of the two body $(K\pi)^o$ system (2 combinations per event).

Fig. 9c: effective mass squared spectrum of the two body $(\pi\pi)$ system.

Fig. 9d: effective mass squared spectrum of the two body $(K_1^oK^{\pm})$ system.

The curves on Fig. 3a, b, c and d correspond to the fit obtained when assuming $K^{*}(891)$, $\rho(765)$ and phase-space contributions.

Fig. 9e: effective mass squared spectrum of the two body $(K_1^o K^{\pm})$ system when $M^2(K\pi) > 0.837$ GeV^2 or $M^2(K\pi) < 0.748$ GeV^2.

The curve on Fig. 3e corresponds to the fit of an S-wave scattering length at threshold and a Breit-Wigner amplitude at $M^2(K_1^o K^{\pm}) = 1.74$ GeV^2.

Fig. 10 $\bar{p}p \to K_1^o K^{\pm} \pi^{\mp} \pi^o$ when $M^2(K_1^o K^{\pm}) < 1.05$ GeV^2.

Fig. 10a: effective mass squared spectrum of the three body $(K_1^o K^{\pm} \pi^{\mp})$ system.

Curve α corresponds to 3-body phase-space when $M^2(K_1^o K^{\pm})$ 1.05 GeV^2. Curve β corresponds to the fit of production of $D^o(1290)$ and phase-space.

Fig. 10b: effective mass squared spectrum of the three body $(K_1^o K^{\pm} \pi^o)$ system.

One sees the difference between the neutral $(K\bar{K}\pi)$ system and the charged one.

REFERENCES

1. Ch. d'Andlau, A. Astier, M. Della Negra, L. Dabrzynski, S. Wojcicki, J. Barlow, T. Jacobsen, L. Montanet, L. Tallone, M. Tomas, A.M. Adamson, M. Baubillier, J. Duboc, M. Goldberg, F. Lévy, D.N. Edwards, J.E.A. Lys, Phys. Lett. 17 (1965) p. 347.

2. R. Armenteros, D.N. Edwards, F. Jacobsen, L. Montanet, J. Vandermeulen, C. d'Andlau, A. Astier, P. Baillon, J. Cohen-Ganouna, C. Defersе, J. Siaud, P. Rivet, International Conference on High Energy Physics, Dubna, 1964, p. 577.

3. P. Baillon's theses. Faculté des Sciences, Paris.

4. The final state $K_1^oK_1^o$ being C = +1 while $K_1^oK_2^o$ is C = -1, the initial states with lowest orbital angular momenta which may contribute to these final states are respectively $3p_0$, $3p_2$, $3F_2$, $3F_4$ on one hand and 3_{S_1}, 3_{D_1}, 3_{D_3} on the other hand.

5. For the $K^{*}(891)$ and $\rho(765)$ amplitudes, we have used the following matrix elements :

$$T_1 = BW_a + BW_b + e^{i\alpha}\,(BW_c + BW_d)\ ;\ T_2 = BW\rho$$

where BW represent normalised Breit-Wigner amplitudes and subscripts (a, b) and (c, d) refer respectively to $(K_1^o\pi^+)$ and $(K_1^o\pi^-)$ combinations. We have established that the fit is not sensitive to the value of α.

6. An attempt was made to fit this data with an additional Breit-Wigner centered at around 1430 MeV. The result of this fit is illustrated by the curve γ on Fig. 7d. Although it gives a better probability (64%), it represents only a two standard deviation effect at M = 1412 $\pm$ 23 MeV with a width of 100 $\pm$ 70 MeV.

7. By S-wave scattering effect, we mean the following parametrisation of the transition amplitude : $\dfrac{1}{1 + ika}$

where k is the momentum of a K_1^o in the $(K\bar{K}$ centre of mass system.

Fig 1

Fig 2

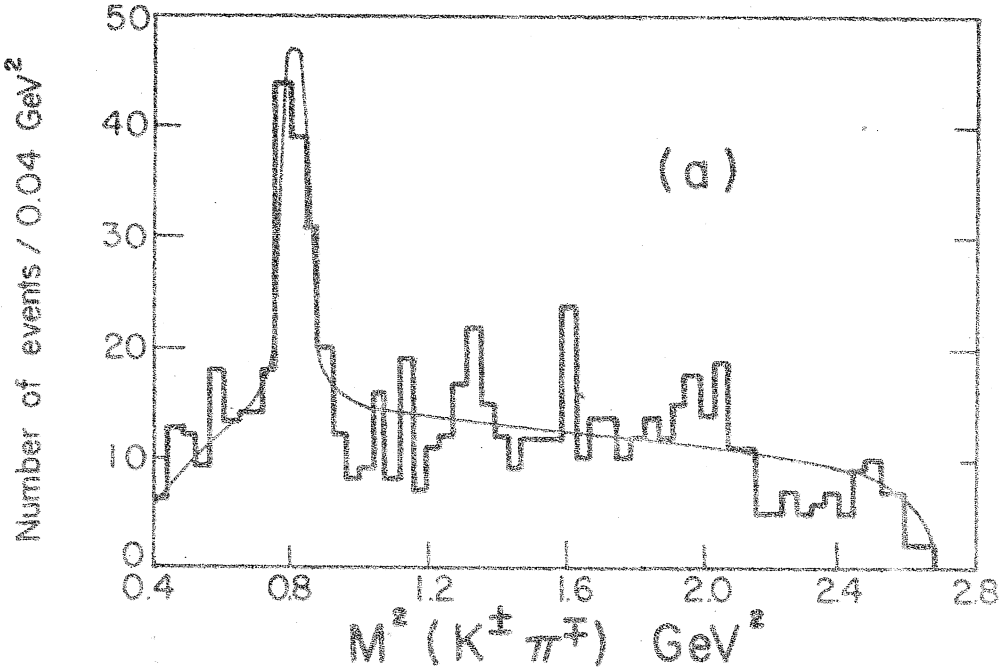
(a)
Number of events / 0.04 GeV²
M² (K± π∓) GeV²

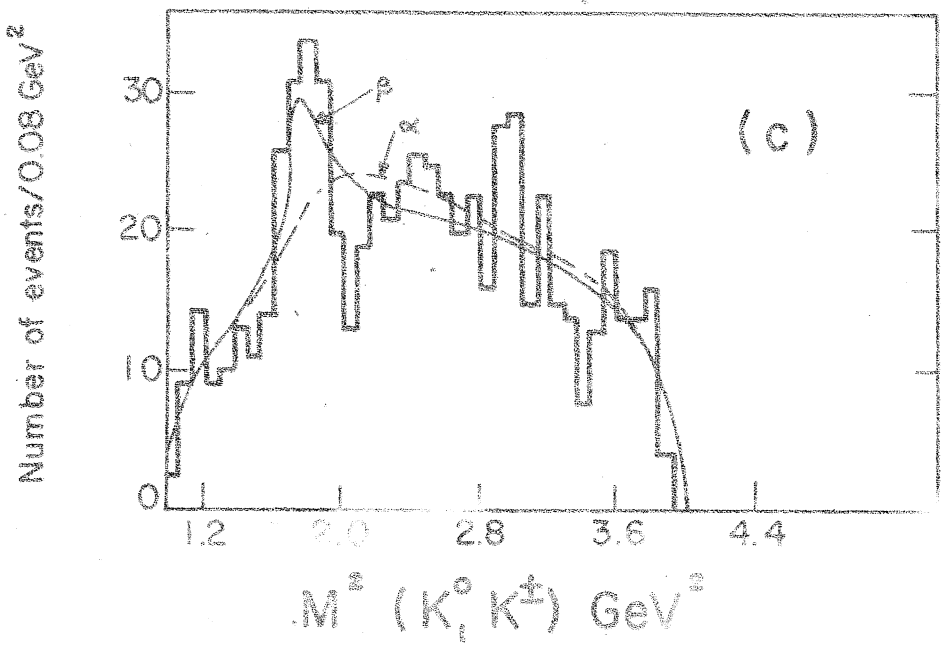
(c)
Number of events/0.08 GeV²
M² (K°, K±) GeV²

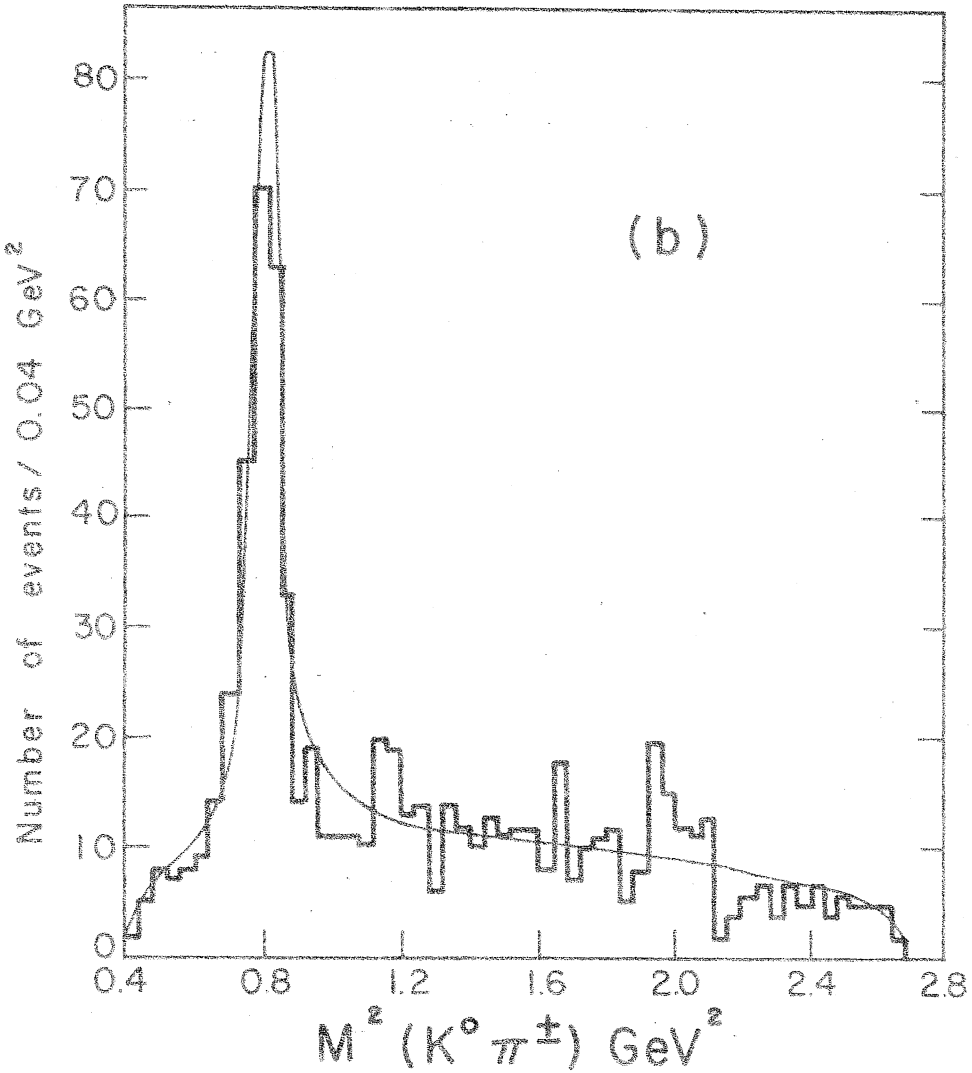
(b)
Number of events / 0.04 GeV²
M² (K° π±) GeV²

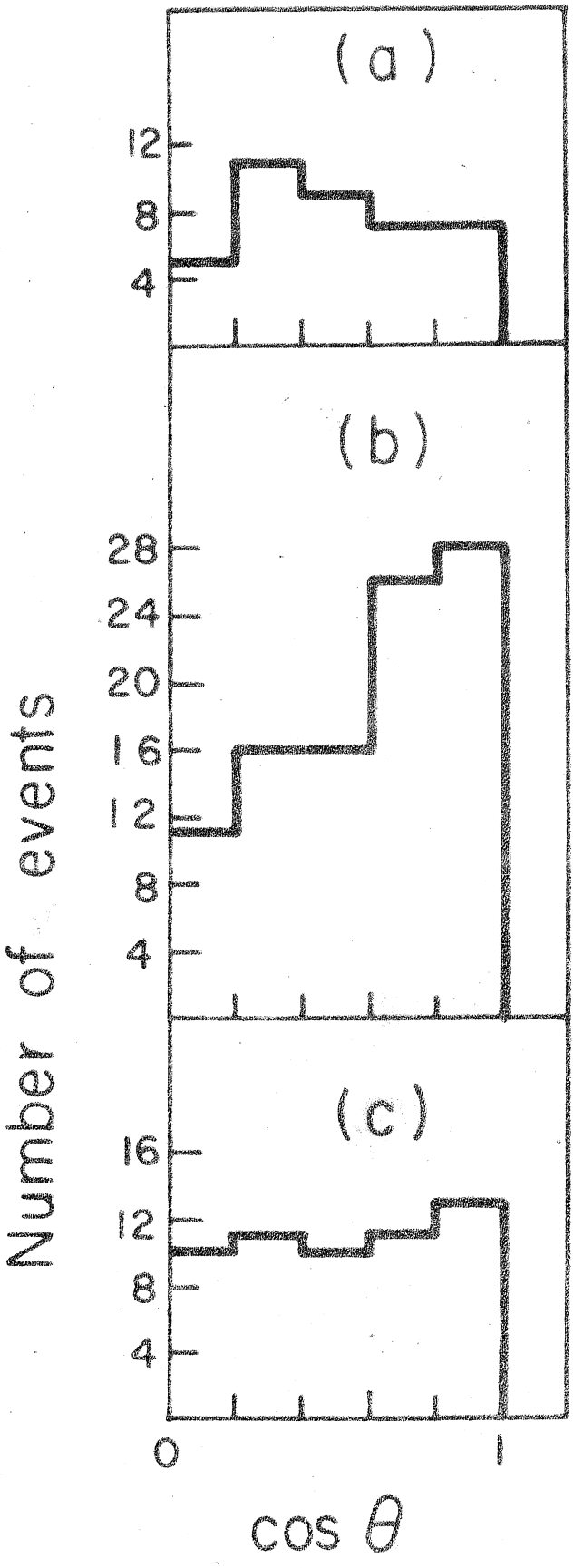
(a)
12
8
4
(b)
28
24
20
16
12
8
4
(c)
16
12
8
4
0
1
Number of events
cos θ

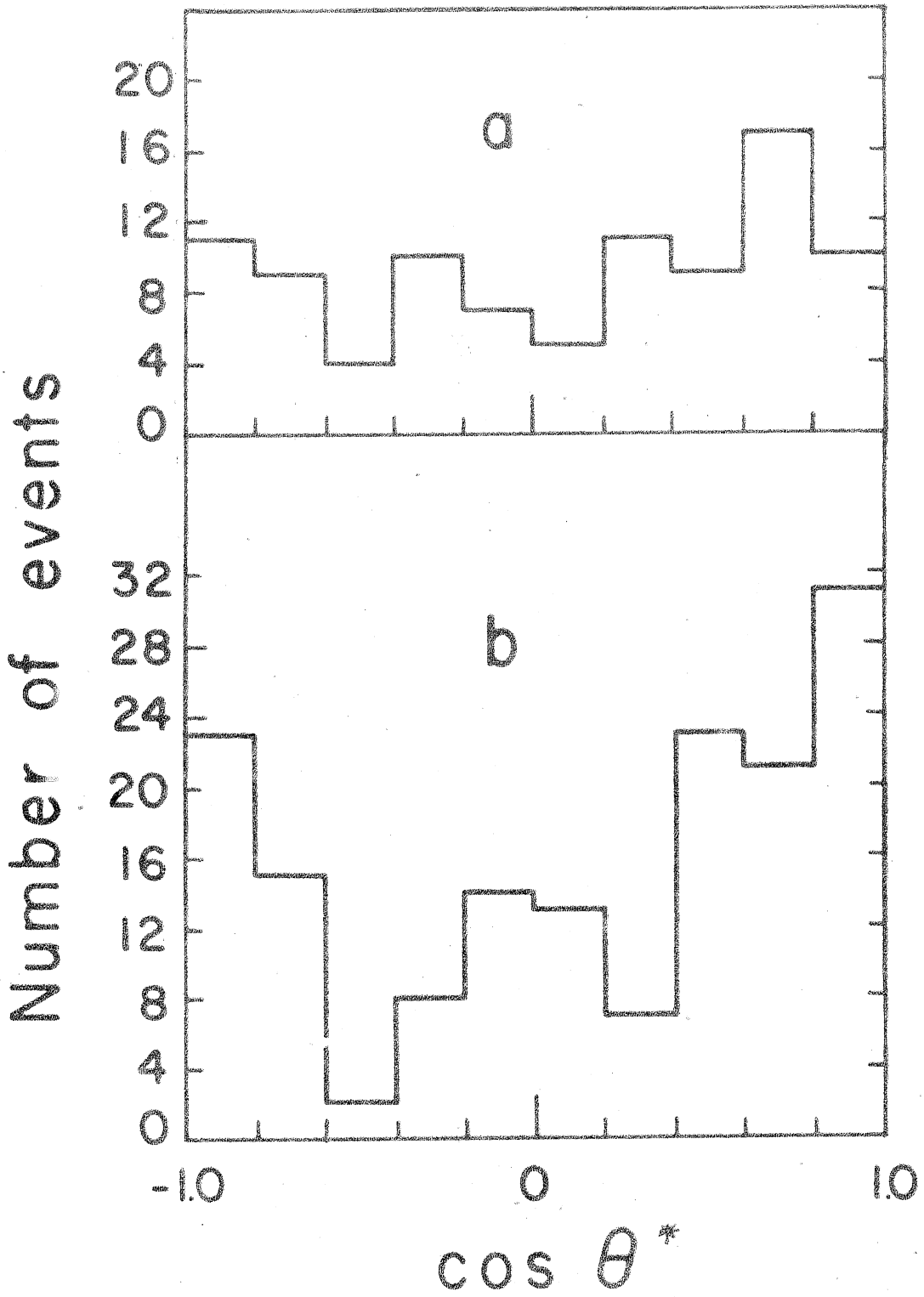

Fig 5

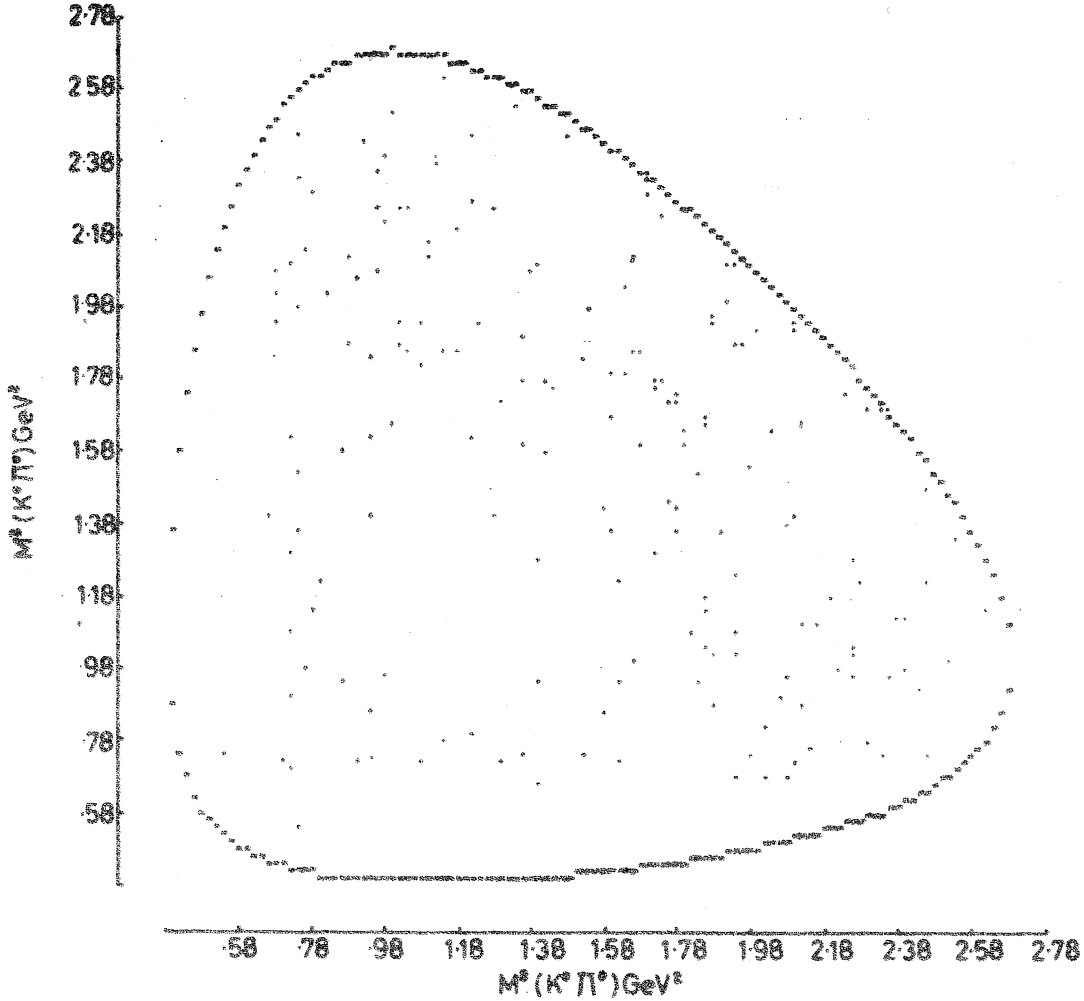
2·78
2·58
2·38
2·18
1·98
1·78
1·58
1·38
1·18
·98
·78
·58
M² (K°π°) GeV²
·58 ·78 ·98 1·18 1·38 1·58 1·78 1·98 2·18 2·38 2·58 2·78
M² (K°π°) GeV²

Fig 6

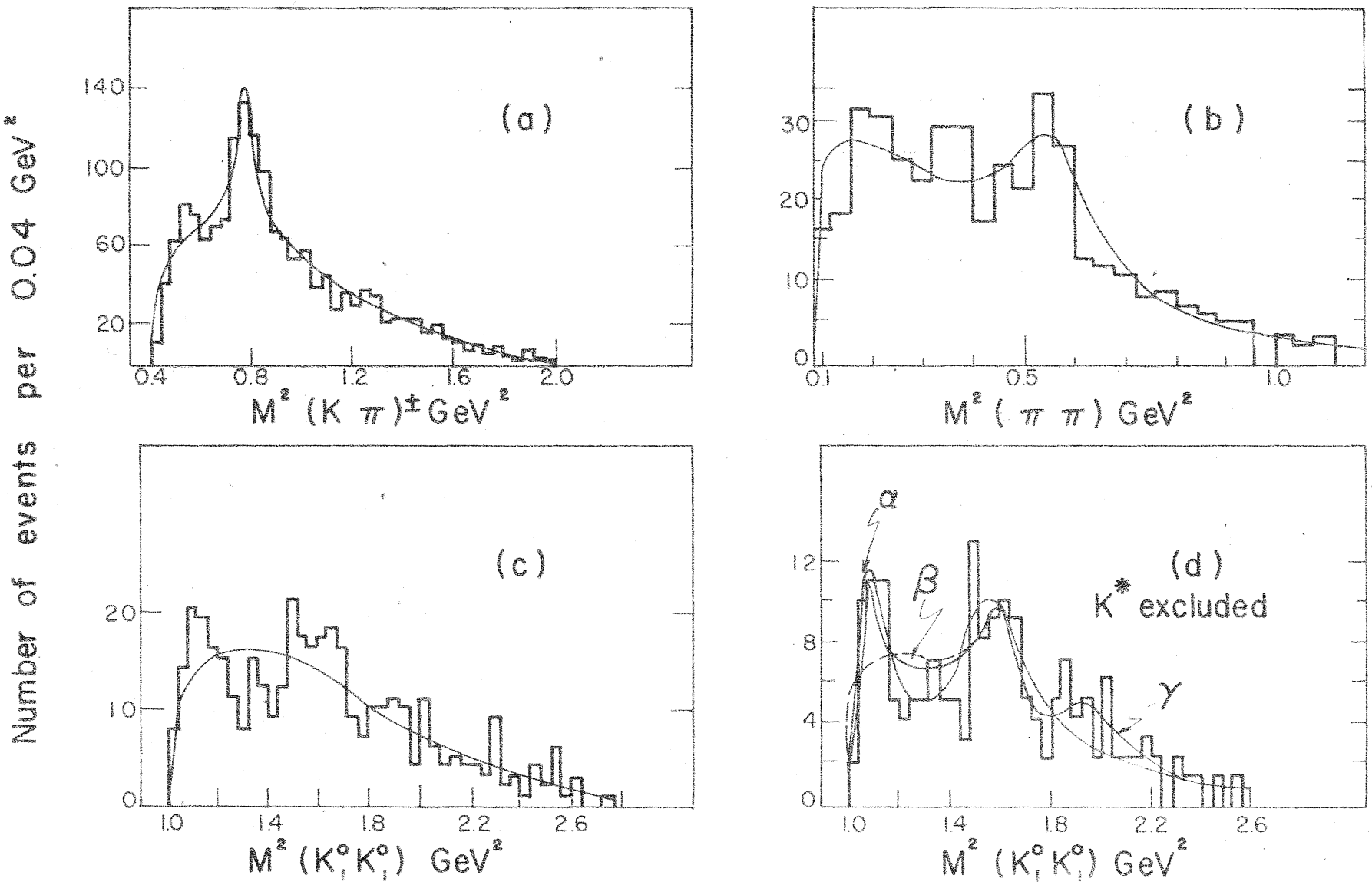
Number of events per 0.04 GeV²
(a)
M² (K π)± GeV²
(b)
M² (π π) GeV²
(c)
M² (K°₁K°₁) GeV²
(d)
K* excluded
α
β
γ
M² (K°₁K°₁) GeV²

Fig 7

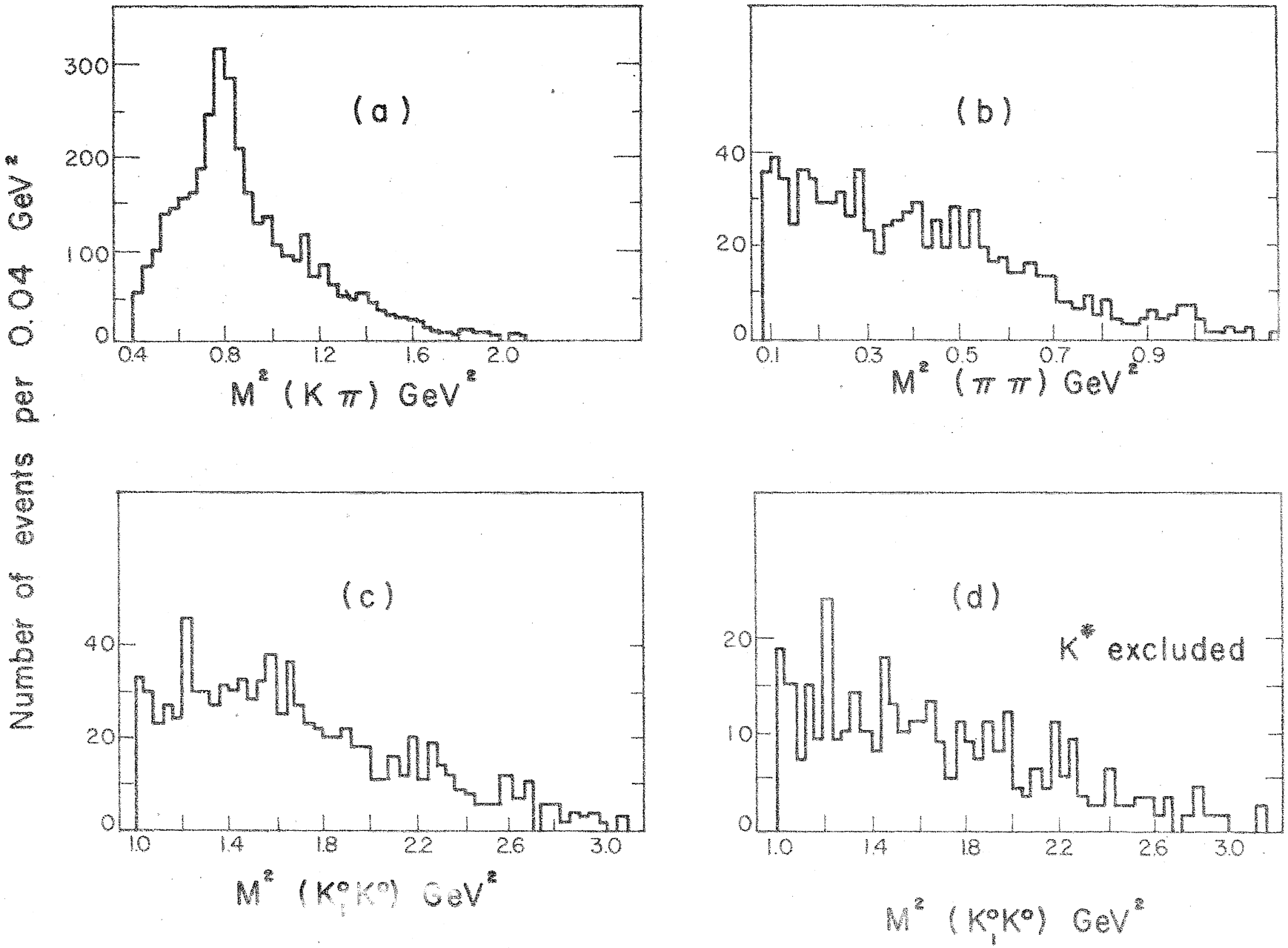
(a)
(b)
(c)
(d)
K* excluded
Number of events per 0.04 GeV²
M² (K π) GeV²
M² (π π) GeV²
M² (K°K°) GeV²
M² (K°K°) GeV²

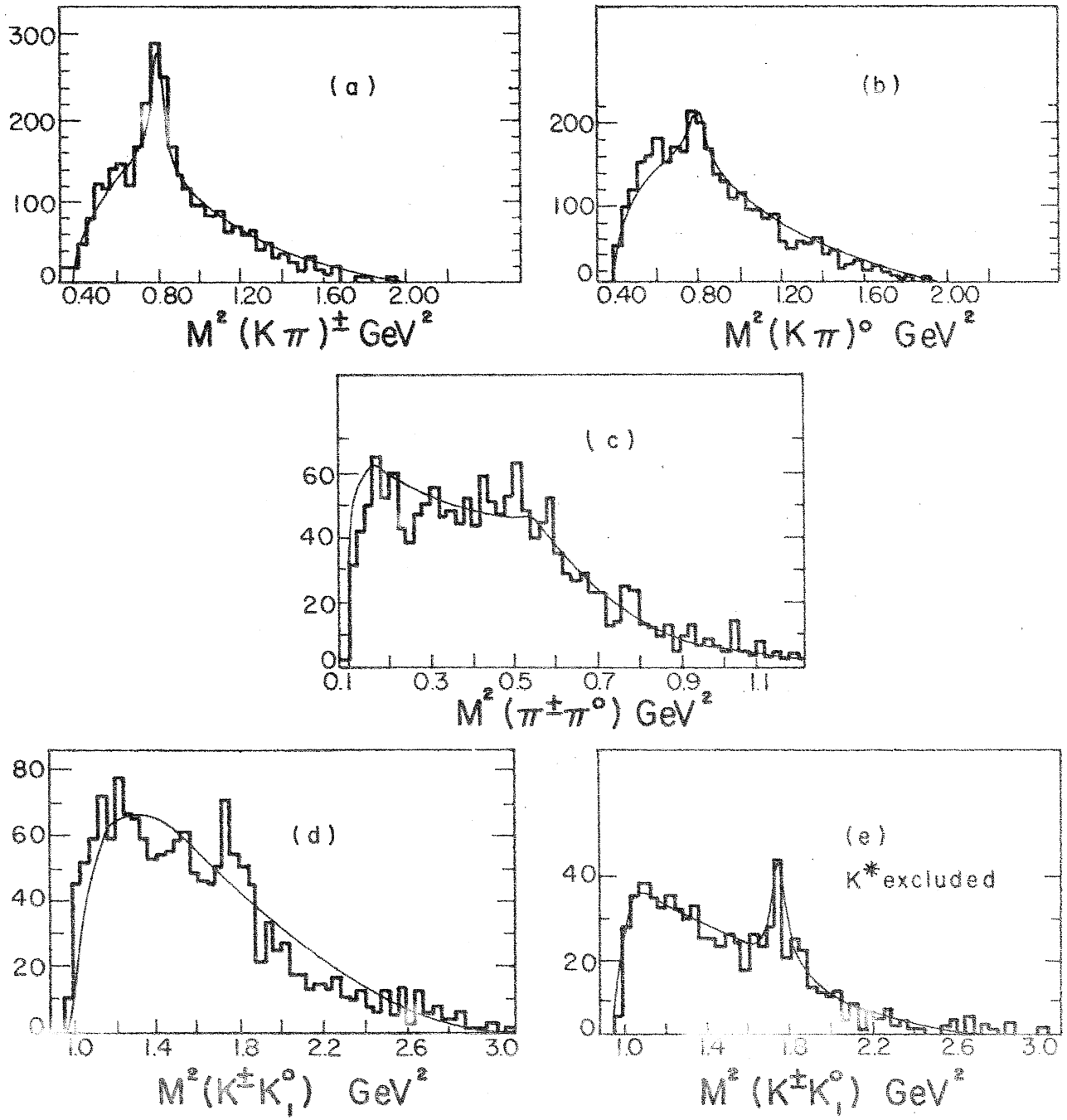
Number of events per 0.04 GeV²
(a)
M² (Kπ)± GeV²
(b)
M²(Kπ)° GeV²
(c)
M² (π±π°) GeV²
(d)
M²(K±K°₁) GeV²
(e)
K* excluded
M² (K±K°₁) GeV²

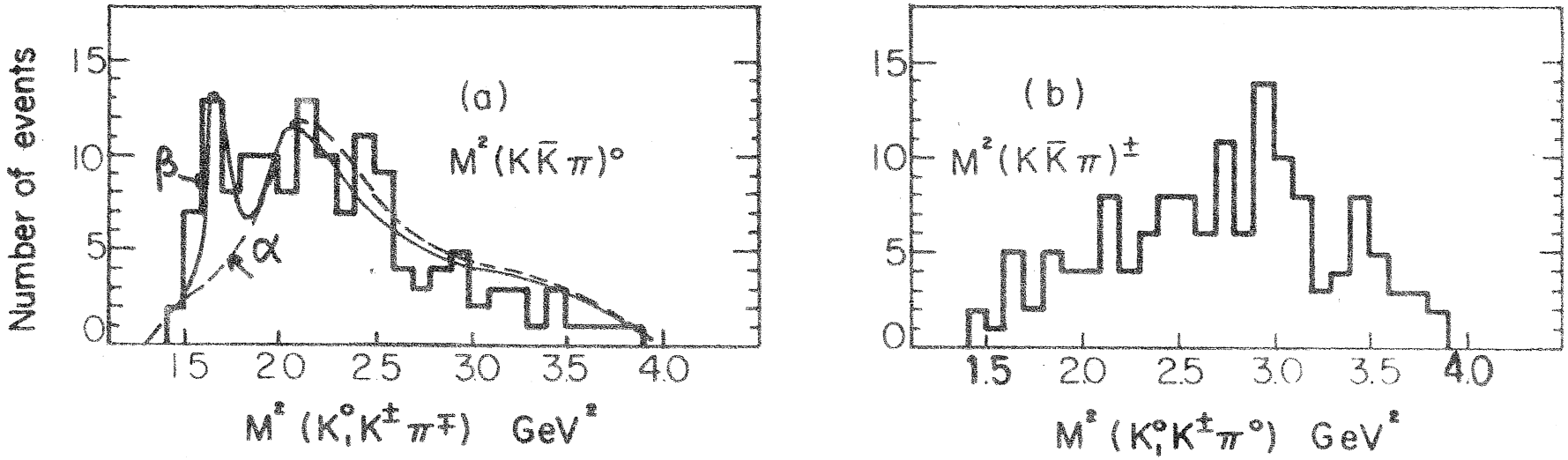

Fig 10